Int. J. Electrochem. Sci., 5 **(2010)** 720 - 730

International Journal of ELECTROCHEMICAL SCIENCE
www.electrochemsci.org

Investigation of sol-gel Synthesized CdO-ZnO Nanocomposite for CO Gas Sensing

Hassan Karami*

Nano Research Laboratory (NRL), Department of Chemistry, Payame Noor University (PNU), P. O. Box: 97, Abhar, Iran
*E-mail: karami_h@yahoo.com

Received: 31 December 2009 / *Accepted:* 15 May 2010 / *Published:* 30 May 2010

A novel CdO-ZnO nanocomposite has been synthesized by a sol-gel pyrrolysis method based on polymeric network of polyvinyl alcohol (PVA). The prepared nanocomposites have been carefully characterized using scanning electron microscopy, X-Ray dispersive energy analysis, ICP-atomic emission spectroscopy and X-Ray diffraction. The obtained results showed that the synthesized nanocomposite at optimum conditions has excellent linear nanoclusters created from nanograins. Each nanograin was made of a CdO core that completely covered by ZnO layers. Each synthesized nanocomposite was used as sensing agent of CO gas. It was found that synthesized CdO-ZnO nanocomposite at 2%wt $Zn(NO_3)_2$, 2%wt $Cd(NO_3)_2$, 9%wt PVA, mixed solvent of 50:50 ethanol-water at pyrrolysis temperature of 600°C can be used as CO gas sensing agent to exhibit the highest sensitivity for CO at 135°C. The constructed sensor showed a very low detection limit of 2 ppm with the dynamic range of 2 to 500 ppm.

Keywords: Nanocomposite, Sol– Gel; ZnO; CdO; Gas Sensor; Carbon monoxide

1. INTRODUCTION

ZnO nanoparticles have received great attention because of their unique catalytic, electrical, gas sensing, optical properties, and a large exciton bonding energy of 60MeV. Their non-toxicity, good electrical, optical, and piezoelectric behavior and other advantages such as their low cost and extensive applications in diverse areas are some of the reasons for this extensive attention. Zinc oxide has proven its diverse usage in different fields of application including, solar cells, photocatalysis, ultraviolet lasers, transparent conductive oxides, spintronics, and gas sensors and etc.

Cadmium oxide (CdO) is a well known II– VI semiconductor with a direct band gap of 2.2 eV (520 nm) and has developed various applications such as its use in solar cells, transparent electrodes, photodiodes, and sensors. There are numerous reports on the synthesis of the nanostructured ZnO through the usage of different methods including the Sol-Gel [1], self-assembly [2], chemical bath deposition [3], emulsion route [4], vapor phase transport [5], reactive sputter [6] and spray-pyrrolysis techniques [7].

There are several reported methods for the preparation of the CdO nanoparticles, but most of these methods only describe the thin film formation of CdO [8]. There is fairly few available literature on the synthesis of the particles as a free-standing powder. Pan et al. reported a formation of several nanobelts at high temperatures from a number of metal oxides; one of them being CdO [9]. Peng et al. reported the formation of CdO nanowires [10]. Recently, the formation of CdO nano-particles using the thermal treatment of cadmium acetate has been described by Ristic et al. [11].

There are numerous reports on the synthesis of various nanocomposites of ZnO with different compounds such as Fe_2O_3 [12], SnO_2 [13] and etc. However, there are no reports on the synthesis of ZnO-CdO composites or nanocomposites.

Several semiconducting oxides such as SnO2, ZnO, In_2O_3 and indium tin oxide (ITO) are employed as gas sensors, by utilizing the changes of the electrical conductivity of these materials upon exposing to target gases [14–18]. The utilization of ZnO in gas sensor applications has a long history. Systems composed mainly of ZnO were studied as chemoresistive materials to detect gases like H_2 [19], NH_3 [20], CH_4 [21], O_2 [22], seafood smell (TMA (trimethylamine)) [23], ethanol [24] and CO [25]. It has been suggested that thin film of ZnO gas sensors exhibit higher sensitivities compared to other forms of ZnO sensors [26]. Carbon monoxide (CO) is one of the most dangerous gases in air pollution and human life. CO is produced by incomplete combustion of fuels and commonly found in the emission of automobile exhausts, the burning of domestic fuels and etc. It is highly toxic and extremely dangerous because it is colorless and odorless. CO sensors are, therefore, required in various situations including the detection of smoldering fires. Nanostructured zinc oxide with diverse morphology of nano-wires, nano-rods and nano-belts has been extensively studied due to its unique physical properties such as wide band gap and large excitonic binding energy and electric conducting properties for applications in short-wavelength optoelectronic devices, solar cells, and sensors [26, 27]. The recent demonstration of gas sensors based on nano-ZnO has further stimulated substantial efforts to explore ZnO nano-structures for high gas sensitivity. However, a nano-ZnO sensor prepared by an arc plasma method did not show an expected high sensitivity even when exposed to CO at a concentration as high as 5000 ppm [27]. Nakamura et al. [28] and Choi [25] reported a sensitivity towards a few hundreds ppm of CO by utilizing CuO– ZnO hetero-contacts, but the grains were not nano-sized. With regards to the combined properties of ZnO and CdO, it is expected that the results of the synthetic CdO-ZnO composite will be interesting. It is expected that composite making can affect on the CO gas sensing ability of ZnO. In this project, we have tried to optimize the synthetic conditions of CdO-ZnO nanocomposite in the linear nanocluster form *via* the poly vinyl alcohol (PVA)-based sol-gel process. CO gas sensing properties of the obtained nanocomposites was studied.

2. EXPERIMENTAL PART

2.1. Materials

All materials were in analytical grade and purchased from Merck, Fluka and or Loba Chimie (India) companies. Double-distilled water was used in all experiments.

2.2. Instrumentals

The morphology and particles diameters of CdO-ZnO nanocomposite samples were studied by a Philips scanning electron microscopy (XL30 model). Powder samples were analyzed by an XRD instrument from Philips Co. (X Per) using the Cu (K_α) radiation and graphite monochrometer. Energy-dispersive X-ray analyses (EDX) were performed by Philips 30 XL. X-ray diffraction (XRD) studies were performed by a Decker D8 instrument. An ICP-AE spectrometer (Varian Vista Pro, CCD Simultaneous, Springvale, Australia) was used for the determination of the zinc and cadmium content of the nanocomposite samples. Gas sensing tests were performed in an isolated box (50cm×40cm×70cm).

2.3. Procedure

2.3.1. Synthesis

In this work, 88 g of a mixed ethanol-water (50:50) solvent was used to dissolve 2 g zinc nitrate, 2 g cadmium nitrate, and 8 g PVA. The mixture was heated to 80°C to form a homogeneous sol solution. The obtained sol was slowly heated to evaporate the solvent and form a hard homogenous gel. The pyrrolysis of the final gel was performed at temperature of 600°C for 8 hours. During the pyrrolysis process, the PVA polymeric network was slowly burnt through the outer surface; zinc and cadmium nitrate salts were simultaneously calcinated and converted into the CdO-CdO nanocomposite. The obtained samples were crushed to prepare a fine powder. The morphology and particles sizes of the samples were analyzed by the SEM, TEM, XRD and EDX. The amount of $Zn(NO_3)_2$, $Cd(NO_3)_2$, PVA, the composition of the mixed solvent, and the pyrrolysis temperature were optimized by the "one at a time method". Response slope and dynamic range were used as the main optimizing parameters. The zinc and cadmium contents of the samples were analyzed by the ICP-AES.

2.3.2. Sensor construction and test

In this study, high resistance polyacrilamide substrates (4 cm × 4 cm × 0.2 cm), prepared with copper interdigitated electrodes were used as sensing device. Fig. 1 shows the sensor configuration.

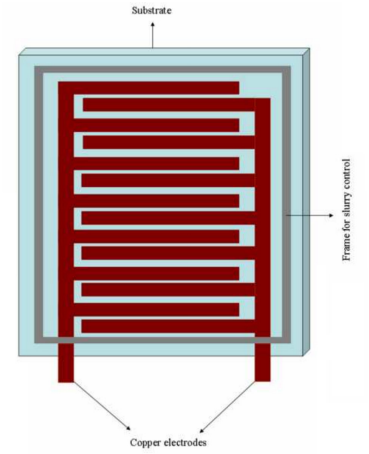

Figure 1. Scheme of used sensor device

The mixture of 1 g nanocomposite in 10 ml acetone was stirred and dispersed by ultrasonic method to give a translucent solution. The homogenous mixture as sensing layer was then screen-printed onto its surface and dried at 120°C for three hours using an oven. Silver paste was used to fix two contact wires. The thickness of the nanocomposite film was measured to be 100 μ m. For sensor test, the sensor chip (Fig. 1) was inserted into the isolated box which filled by N_2 gas. The temperature of sensor chip was adjusted in 135 °C and a constant voltage of 60 V was applied by a power supply instrument into the two output wires of sensor chip. Finally, different amounts of CO gas were injected into the box. Internal atmosphere of the box was circulated by a small fan to make a homogenous gas. After stabilizing, the current of sensor circuit was determined by a high sensitive galvanometer. The determined current was related to the electrical resistance of the sensor. The sensor resistance was related to the CO concentration in the box.

3. RESULTS AND DISCUSSION

3.1. Synthetic optimization

In the proposed method, the gel network rigidity controls the morphology and particle size of the synthesized sample to make a uniform nanostructured CdO-ZnO composite. In the gel structure, cadmium and zinc salts were homogeneously dispersed among polymeric network. Because of gel network rigidity, the dispersed ions in the gel network can not alter their positions. Therefore, during the pyrrolysis of the gel's outer layers, the zinc and cadmium ions of the burnt layers combine with each other to create the double salts of $Cd(NO_3)_2$ and $Zn(NO_3)_2$ which also react to yield CdO-ZnO nanocomposite. The chemical equation is as follows:

$$Cd(NO_3)_2.Zn(NO_3)_2 \xrightarrow{Heat} CdO.ZnO + 4NO_2$$

In this method, the amount of $Zn(NO_3)_2$, $Cd(NO_3)_2$, PVA, the mixed solvent composition, and the pyrrolysis temperature have an affect on the composition, morphology, and particle size of the sample. The degree of these effects was optimized by the "one at a time" method. In the first step of the optimization process of synthetic conditions, the pyrrolysis temperature was varied from 400°C to 850°C. The synthesized samples were studied by the SEM and EDX instruments. The results showed that the use of a pyrrolysis temperature which is lower than 550°C not only has no considerable effect on the composition, morphology, or particle size, but also caused a longer pyrrolysis time (more than 12 h). On the other hand, the use of a temperature higher than 600°C caused the formation of agglomerated structures and bigger particles. This led to the selection of a 600°C pyrrolysis temperature as an optimum temperature for future studies. For additional confirming, each sample was used as CO gas sensing agent. The obtained results of sensor studies showed that the sample synthesized at 600°C pyrrolysis temperature has wide dynamic range and high response slope. Table 1 shows the synthetic conditions and EDX results for optimization set.

Table 1. Experimental conditions of the synthesized samples and EDX results of each sample

Experiment No.	%wt			Ethanol:water (V:V)	EDAX results (%wt)	
	$Zn(NO_3)_2$	$Cd(NO_3)_2$	PVA		CdO	ZnO
1	0.5	0.5	9	50:50	0.93	99.07
2	1	1	9	50:50	0.74	99.26
3	2	2	9	50:50	0.62	99.38
4	4	4	9	50:50	1.42	98.58
5	6	6	9	50:50	73.86	26.14
6	1	2	9	50:50	0.62	99.38
7	2	1	9	50:50	0.86	99.14
8	2	3	9	50:50	1.01	98.99
9	3	2	9	50:50	1.25	98.75
10	2	2	0	50:50	49.50	50.50
11	2	2	1	50:50	2.05	97.95
12	2	2	3	50:50	1.62	98.38
13	2	2	5	50:50	2.21	97.79
14	2	2	7	50:50	0.95	91.05
15	2	2	9	50:50	2.5	97.5
16	2	2	11	50:50	5.2	94.8
17	2	2	13	50:50	8.5	91.5
18	2	2	9	100:0	1.0	99.0
19	2	2	9	75:25	2.4	97.6
20	2	2	9	50:50	0.62	99.38
21	2	2	9	25:75	15.91	84.09
22	2	2	9	0:100	43.89	56.11

Experiments 1 to 9 were used to optimize the weight percentages of cadmium and zinc nitrates in the initial sol. Experiments 10 to 17 were a set for optimization of the PVA amount. The last set of experiments, i.e. 18 to 22, was performed to optimize the mixed solvent composition. Each synthesized sample was studied by SEM and EDX. The experimental optimization set was performed to obtain a uniform nanostructure for the CdO-ZnO nanocomposite, and also high response slope and wide dynamic range for the constructed sensors. The obtained results showed that by varying each of the parameters mentioned in Table 1, the morphology, particle size, components of the synthesized samples and sensor abilities changed. The optimum conditions for synthesis of a uniform nanostructured CdO-ZnO composite with high response slope and wide dynamic range for its sensor includes 2 %wt $Zn(NO_3)_2$, 2 %wt $Cd(NO_3)_2$, 9 %wt PVA, and a mixed solvent of 50:50 ethanol-water. Figure 2 shows the EDX analysis and SEM images of the sample which synthesized in the optimum conditions in two magnifications of 15000 (Fig. 2b) and 30000 (Fig. 2c). As it is seen in Fig. 2, the optimum sample has a perfect uniform nanostructure in a linear cluster shape. Each linear nanocluster has been formed from several uniform spherical grains (seeds) with 70 to 90 nm in diameter.

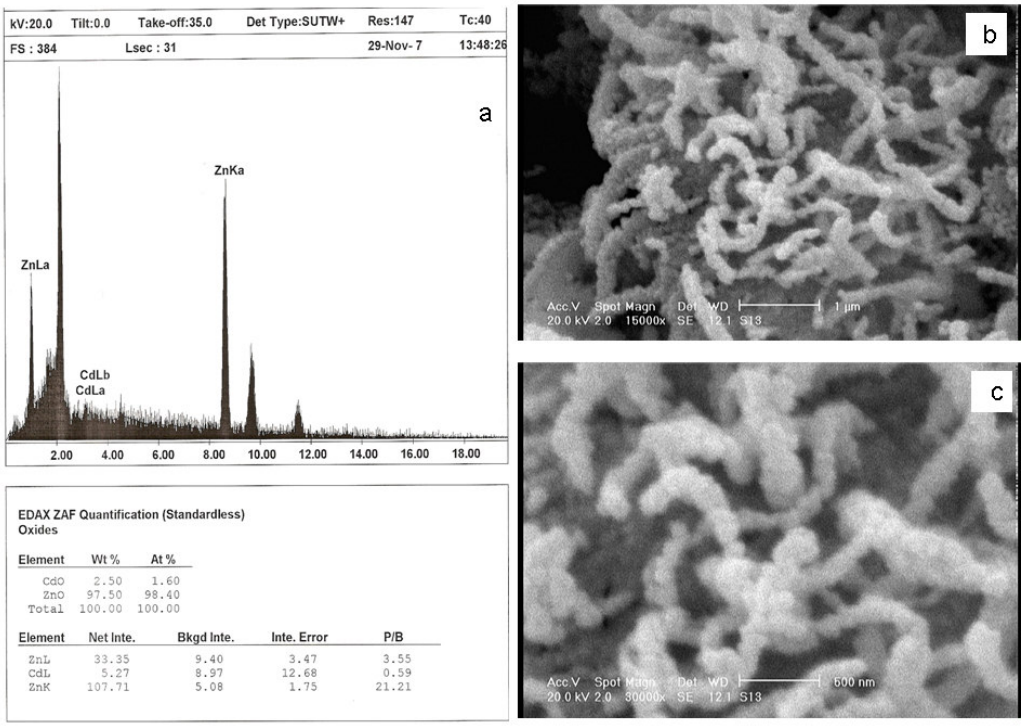

Figure 2. EDX analysis and SEM images of the synthesized sample in the optimum conditions including 2 %wt Zn(NO3)2, 2 %wt Cd(NO3)2, 9 %wt PVA, mixed solvent of 50:50 ethanol-water and pyrrolysis temperature of 600°C; EDX analysis (a), SEM image in magnifications of 15000 X (b) and in magnification of 30000 X (c)

The EDX analysis results shows that in the major experiments mentioned in Table 1(eg: the optimum synthesis; Fig. 2a), the CdO content in the surface layers of the nanocomposites was

insignificant. It should be mentioned that the EDX method only nalyzes the surface of particles, therefore, in each nanocomposite bead (grains of linear nanoclustes); CdO forms the core and is then covered by ZnO. Some of these samples were analyzed by XRD which results confirmed the EDX analysis results. If this hypothesis is correct, not only will the bulk analysis of sample using a ICP-Atomic emission spectroscopy (ICP-AES) show that the amount of Cd in the nanocomposite is not negligible but also, the weight ratio of Cd/Zn would be the same with that of what was in the initial sol. In order to investigate the hypothesis, some samples that had shown insignificant amounts of CdO in the EDX analysis were analyzed by the ICP-AES. The ICP-AES results showed that the cadmium and zinc contents of the samples were the same as their initial concentrations in the sol. The hypothesis of ZnO covering the CdO seed was therefore confirmed. Figure 3 shows the suggested structure for the CdO-ZnO nanocomposite.

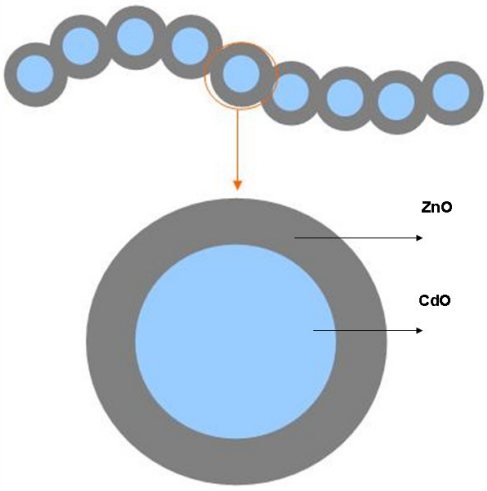

Figure 3. Scheme of the suggested structure for the CdO-ZnO nanocomposite

3.2. Optimization of CO gas sensing

After optimization of synthetic conditions of the CdO-ZnO nanocomposite to obtain high response slope, wide dynamic range and uniform morphology, sensing conditions were exactly investigated. For this propose thickness of screen-printed layer, sintering temperature, sensing temperature and operating voltage was optimized by the "one at a time method".

Table 2 summarizes the experimental data for optimization set. Based on the Table 2, sensor performance is improved when screen-printed layer thickness is increased from 10 to 100 μ. This result is due to complete substrate covering. At higher thickness, film resistance will be increased.

About the effect of sintering temperature, connection between nanocomposite particles is not complete at lower temperatures so that the sensor ability is low. Sensor performance is decreased at temperatures higher than 120°C. The result can be related to decrease porosity of the film.

Table 2. Experimental data for optimizing of CO sensing

Experiment No.	Initial factor				Optimizing parameter	
	Film thickness (μ)	Sintering temperature (°C)	Sensing temperature (°C)	Operating voltage (V)	Detection limit (ppm)	Dynamic range (ppm)
1	***10***	120	130	30	40	40-120
2	***40***	120	130	30	23	23-130
3	***70***	120	130	30	13	13-200
4	***90***	120	130	30	8	8-400
5	***100***	120	130	30	***7***	***7-446***
6	***110***	120	130	30	8	8-444
7	***150***	120	130	30	10	10-440
8	***250***	120	130	30	17	17-260
9	***400***	120	130	30	20	20-150
10	100	***80***	130	30	40	40-135
11	100	***90***	130	30	25	25-157
12	100	***100***	130	30	15	15-200
13	100	***110***	130	30	11	11-380
14	100	***120***	130	30	***7***	***7-446***
15	100	***130***	130	30	7	7-450
16	100	***140***	130	30	10	10-411
17	100	120	***100***	30	30	30-210
18	100	120	***110***	30	20	20-300
19	100	120	***120***	30	15	15-410
20	100	120	***130***	30	7	7-450
21	100	120	***135***	30	***4***	***4-480***
22	100	120	***140***	30	5	5-420
23	100	120	***145***	30	5	5-412
24	100	120	135	***20***	5	5-410
25	100	120	135	***30***	4	4-490
26	100	120	135	***40***	3	3-495
27	100	120	135	***50***	***2***	***2-500***
28	100	120	135	***60***	3	3-490

Table 2 shows that 135 °C is the optimum value for sensing temperature. Sensor sensitivity is strongly depended on temperature, because CO adsorption/desorption kinetics is increased by the temperature. At higher temperature than 135°C, CO adsorption is decreased. Operating voltage is related to sensor sensitivity. Increasing of the operating voltage causes to increase circuit current. The circuit current directly relates the slope of sensor response. At this type sensor, high slope makes lower detection limit.

In summary, for CO sensing, film thickness 100 μ, sintering temperature 120°C, sensing temperature 135°C and operating voltage 50 V are optimum values to obtain low detection limit, wide dynamic range and high response slope.

3.3. Sensor specifications

Figure 4 shows the effect of CO concentration on the sensor response. As it can be seen from Fig. 4, the constructed sensor has a wide dynamic range (2-500 ppm), low detection limit (2 ppm) and high sensitivity (0.1 Ohm.ppm^{-1}).

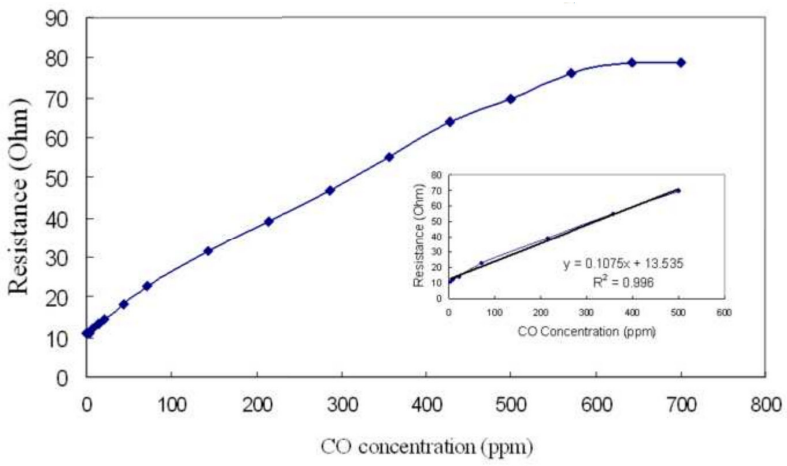

Figure 4. Response curve of the proposed sensor for different concentration of CO with inserted linear calibration curve

Figure 5 shows the response time curve for the proposed sensor. As it is obvious in Fig. 5, at major concentrations, response time is lower than 50 s. The obtained result shows sensor ability to detect CO gas at flow systems.

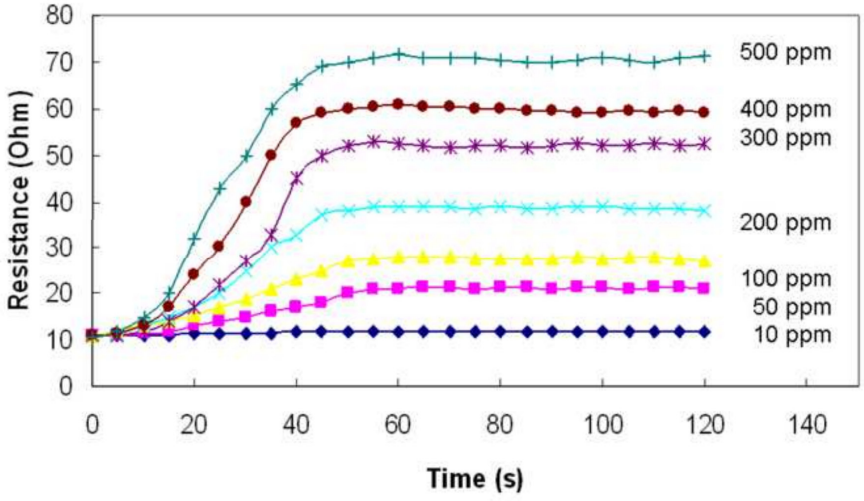

Figure 5. Sensor response time for the different CO concentrations

Selectivity is an important parameter in all gas sensing systems. Sensor selectivity was studied for some gas molecules of air. Figure 6 shows the effect of some interfering gas molecules on the CO sensor response. As it can be seen from Fig. 6, the proposed sensor is a selective sensor in dry atmosphere. Humidity has considerable interference on the CO sensor, so that, the sensor can be used as humidity sensing device at clean air (without CO or CO with low concentration).

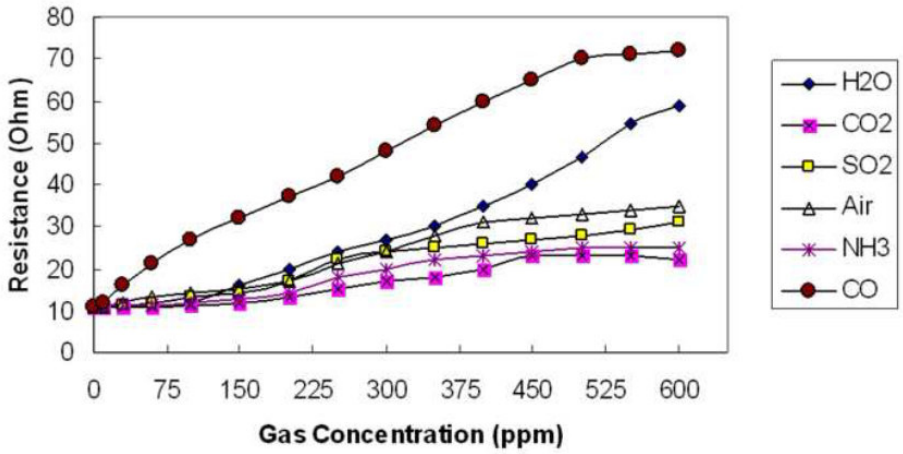

Figure 6. Effect of some interfering gases on the CO sensor

Comparing of the proposed sensor as CO gas sensing device with the previously reports shows that the proposed sensor has higher efficiency [13, 19, 23, 25, 28]. The obtained results showed that making composite causes much improvement in sensor performance in comparing with doping and other modifications.

4. CONCLUSIONS

PVA-based sol-gel pyrrolysis method can be used as a useful method to synthesize the CdO-ZnO nanocomposite. This method synthesizes the optimum nanoclusters formed from the linear connections of a great number of spherical nanograins (nanoseeds) with each nanograin's diameter varying from 70 to 90 nm. The optimized nanocomposite exhibits good ability to detect CO gas.

ACKNOWLEDGEMENTS
We gratefully acknowledge the support of Abhar Payame Noor University Research Council, throughout these research experiments.

References

1. A. Trinchi Y. X. Li, W. Wlodarski, S. Kaciulis, L. Pandolfi, S. P. Russo, J. Duplessis and S. Viticoli, *Sens Actuators A* 108 (2003) 108.
2. H. A. Ali, A. A. Iliadis, R. F. Mulligan, A. V. W. Cresce, P. Kofinas and U. Lee, *Solid State Electron* 46 (2002)1639.
3. V. R. Shinde, T. P. Gujar, C. D. Lokhande, R. S. Maneb and S. H. Han, *Mater Scie Engin B* 137 (2007) 119.
4. Y. He, *Appl Surf Scie* 249 (2005) 1.
5. K. Yu, Y. Zhang, R. Xu, D. Jiang, L. Luo, Q. Li, Z. Zhu and W. Lu, *Solid State Commun* 133 (2005) 43.
6. B. S. Jeong, J. D. Budai and D. P. Norton, *Thin Solid Film* 422 (2002) 166.
7. S. H. Keshmiri and M. R. Rokn-Abadi, *Thin Solid Film* 382 (2001) 230.
8. D. Ma, Z. Ye, L. Wang, J. Huang and B. Zhao, *Mater Lett* 58 (2003) 128.
9. Z. W. Pan, Z. R. Dai and Z. L. Wang, *Science* 291 (2001) 1947.
10. X. S. Peng, X. F. Wang, Y. W. Wang, C. Z. Wang, G. W. Meng and L. D. Zhang, *Appl Phys* 35 (2002) L101.
11. M. Ristic, S. Popovic and S. Music, *Mater Lett* 58 (2004) 2494.
12. H. Tang, M. Yan, H. Zhang, S. Li, X. Ma, M. Wang and D. Yang, *Sens Actuators B* 114 (2006) 910.
13. L. C. Tien, D. P. Norton, B. P. Gila, S. J. Pearton, H. T. Wang, B. S. Kang and F. Ren, *Appl Surf Scie* 253 (2007) 4748.
14. D. H. Yoon and G. M. Choi, *Sens. Actuators B* 45 (1997) 251.
15. M. C. Horrillo, A. Serventi, D. Rickerby and J. Gueierrez, *Sens. Actuators B* 58 (1999) 474.
16. C. A. Papadopoulos, D. S. Vlachos and J. N. Avaritsiotis, *Sens. Actuators B* 42 (1997) 95.
17. G. Sberveglieri, G. Faglia, S. Groppelli and P. Nelli, *Sens. Actuators B* 8 (1992) 79.
18. T. Seiyama and S. Kagawa, *Anal. Chem.* 38 (1966) 1069.
19. B. Bott, T.A. Jones and B. Mann, *Sens. Actuators* 5 (1984) 65.
20. H. Nanto, T. Minami and S. Takata, *J. Appl. Phys*. 60 (1986) 482.
21. M. Egashira, N. Kanehara, Y. Shimizu and H. Iwanaga, *Sens Actuators B* 18 (1989) 349.
22. G. Sberveglieri, P. Nelli and S. Groppelli, *Mater. Sci. Eng. B* 7 (1990) 63.
23. H. Nanto, H. Sokooshi and T. Kawai, *Sens. Actuators B* 14 (1993) 715.
24. D. F. Paraguay, M. Miki-Yoshida, J. Morales, J. Solis and L.W. Estrada, *Thin Solid Films* 373 (2000) 137.
25. J. D. Choi and G. M. Choi, *Sens. Actuators B* 69 (2000) 120.
26. A. K. Mukhopadhyay, P. Mitra, D. Chattopadhyay and H. S. Maiti, *J. Mater. Sci. Lett.* 15 (1996) 431.
27. L. F. Dong, Z. L. Cui and Z. K. Zhang, *NanoStruct. Mater* 8 (1997) 815.
28. Y. Nakamura, H. Yoshioka, M. Miyayama, H. Yanagida, T. Tsurutani and Y. Nakamura, *J. Electrochem. Soc.* 137 (1990) 940.